

GY4137, a hydrogen sulfide (H₂S) donor, shows potent anti-hepatocellular carcinoma activity through blocking the STAT3 pathway

SEN LU, YUN GAO, XINLI HUANG and XUEHAO WANG

Center of Liver Transplantation, The First Affiliated Hospital of Nanjing Medical University, The Key Laboratory of Living Donor Liver Transplantation, Ministry of Health, Nanjing 210029, P.R. China

Received November 6, 2013; Accepted December 19, 2013

DOI: 10.3892/ijo.2014.2305

Abstract. GYY4137, a hydrogen sulfide (H₂S) donor, exhibits anticancer activity by a combination of cell cycle arrest and promoting apoptosis, and inhibits tumor growth, however, the precise mechanisms involved remain unclear. In this study, we discovered that GYY4137-mediated suppression of cell proliferation in human hepatocellular carcinoma (HCC) cell lines and tumor growth in a subcutaneous HepG2 xenograft model may be due to directly targeting the signal transducer and activator of transcription 3 (STAT3) pathway. We found that GYY4137 suppressed STAT3 activation by reducing p-STAT3 (Y705) levels effectively in HepG2 and Bel7402 cells. Altered expression levels of STAT3-regulated downstream proteins including Bcl-2, cyclin D1, Mcl-1, survivin, vascular endothelial growth factor (VEGF) and hypoxia-inducible factor-1 α (HIF-1 α) may contribute to the inhibition of G1/S cell cycle transition and angiogenesis. Increased cleaved caspase-9, caspase-3 and poly(ADP-ribose) polymerase (PARP) cleavage may induce cell apoptosis in HepG2 and Bel7402 cells. *In vivo*, GYY4137 significantly inhibited tumor growth in the subcutaneous HepG2 xenograft model by inhibiting STAT3 activation and its target gene expression. These results suggest that GYY4137-mediated suppression of HCC growth may be due to the inhibition of the STAT3 pathway.

Introduction

Hepatocellular carcinoma (HCC) is the second leading cause of cancer-related deaths worldwide, with the average annual incidence on the rise both in China and elsewhere (1). The increasing knowledge in the molecular pathogenesis of HCC, as well as the introduction of molecular targeted therapies in oncology, has created an encouraging trend in the management

of this malignancy. Most HCC treatments are designed to abrogate signaling pathways related to cancer cell proliferation, cell survival, angiogenesis, invasion and metastasis (2,3). Signal transducer and activator of transcription 3 (STAT3), a major transducer to mediate the signal from interleukin-6 (IL-6) to the nucleus, may be involved in oncogenesis, cell proliferation, angiogenesis, immune evasion and apoptotic resistance (4-8). IL-6 induces STAT3 phosphorylation at tyrosine residue 705 through Janus-activated kinase (JAK) (9). STAT3 phosphorylation results in homodimerization or heterodimerization of STAT3, enabling nuclear localization and DNA binding, and regulating downstream genes involved in controlling cell cycle progression and programmed cell death (e.g., Bcl-2, cyclin D1, Mcl-1 and survivin) (10), and in the regulation of angiogenesis [e.g., vascular endothelial growth factor (VEGF) and hypoxia-inducible factor-1 α (HIF-1 α)] (4). The inhibition of aberrant STAT3 activation by genetic or pharmacological approaches has repeatedly been demonstrated to result in growth inhibition, apoptosis *in vitro* (11,12), as well as tumor growth and metastasis inhibition *in vivo* (12-14) in HCC. STAT3 is significantly correlated with the prognosis of HCC patients (8,15), indicating that IL-6/STAT3 signaling pathway might be a therapeutic target.

The potential biological significance of hydrogen sulfide (H₂S) has attracted growing interest in recent years. A number of studies have investigated the role of H₂S in triggering cell death and evidence has been presented that this gas can affect cancer cell survival using sulfide salts as donor agents (16,17). The slow-releasing H₂S donor, GYY4137, exhibits anticancer activity by releasing H₂S down slowly (18). It exhibits anticancer activity by a combination of cell cycle arrest and promoting apoptosis, inhibits tumor growth (18), however, the precise mechanism(s) involved remain unclear. Recent study reported that GYY4137 exhibited anti-inflammatory effect *in vivo* and *in vitro* (18,19). We propose that the anticancer activity of GYY4137 may be relative with its suppression of IL-6/STAT3 pathway.

We therefore sought to investigate whether GYY4137 is efficacious for treatment of HCC with a particular focus on its suppression of IL-6/STAT3 pathway. We found that GYY4137 blocked IL-6-induced STAT3 cascade leading to the suppression of cell growth, induction of cell apoptosis and

Correspondence to: Dr Xuehao Wang, Center of Liver Transplantation, The First Affiliated Hospital of Nanjing Medical University, 300 Guangzhou Rd., Nanjing 210029, P.R. China
E-mail: wangxuehao2013@126.com

Key words: GYY4137, hydrogen sulfide donor, hepatocellular carcinoma, STAT3 pathway

cell cycle arrest. GYY4137 also inhibited tumor growth and STAT3 activation in a subcutaneous xenograft model with HepG2 cells *in vivo*. These results suggest that GYY4137 may be a candidate for HCC therapy through blocking constitutive STAT3 signaling.

Materials and methods

Materials. GYY4137 was obtained from the National Institute for the Control of Pharmaceutical and Biological Products (Beijing, China). STAT3, p-STAT3 (Y705), p-STAT3 (S727), JAK, p-JAK2, Bcl-2, Mcl-1, cyclin D1, survivin, HIF-1 α , VEGF, cleaved-poly(ADP-ribose) polymerase (PARP), cleaved-caspase-9 and cleaved-caspase-3 antibodies were purchased from Cell Signaling Technology (Beverly, MA, USA). β -actin antibody was purchased from Sigma (St. Louis, MO, USA). 3-(4,5-dimethyl-2-thiazolyl)-2,5-diphenyl-2H-tetrazolium bromide (MTT), RNase and sodium-orthovanadate and propidium iodide (PI) was purchased from Sigma-Aldrich (St. Louis, MO, USA).

Cell lines and cultures. HCC cell lines HepG2, and Bel7402, and hepatocellular LO2 cells were obtained from the Cell Bank of the Shanghai Institute of Biochemistry and Cell Biology were maintained in RPMI-1640 medium (Invitrogen, Carlsbad, CA) supplemented with 10% fetal bovine serum (FBS) (Invitrogen). All cells were cultured in a humidified atmosphere with a 5% CO₂ incubator at 37°C.

Cell viability assay. HepG2, Bel7402 and LO2 cells were incubated in triplicate in a 96-well plate at a density of 1x10⁴ cells with 100 μ l culture medium per well in the presence or absence of indicated concentrations of GYY4137 for 24, 48 and 72 h. After which, cell viability was determined by the MTT dye uptake method as described earlier (20).

Western blot analysis. HepG2 and Bel7402 cells were cultured in 6-well plates at a density of 5x10⁵ cells/ml in a CO₂ incubator overnight and treated with GYY4137. The total protein was prepared as previously described (21). The equalized amounts of proteins from each sample were subjected to sodium dodecyl sulfate polyacrylamide gel electrophoresis (SDS-PAGE) followed by transfer to polyvinylidene fluoride (PVDF) membranes. The membranes were blocked in 1% (w/v) bovine serum albumin (BSA) for 2 h, and then incubated with the primary antibody overnight at 4°C. Primary antibodies were STAT3, p-STAT3 (Y705), p-STAT3 (S727), JAK2, p-JAK2 (Y1007/1008), Bcl-2, Mcl-1, cyclin D1, survivin, HIF-1 α , VEGF, cleaved-PARP, cleaved-caspase-9, cleaved-caspase-3 (Cell Signaling Technology) and β -actin (Sigma). Then the membranes were incubated with secondary antibody conjugated with IgG horseradish peroxidase (HRP) for 1 h at room temperature and immune complexes were detected by the enhanced chemiluminescence system. β -actin served as a loading control.

Cell cycle analysis. HepG2 and Bel7402 cells were incubated in 6-well plates in the presence of different concentrations of GYY4137 for 24 h. Thereafter, treated cells were fixed and incubated with RNase and propidium iodide (PI) in PBS.

Cell cycle distribution was analyzed with a FACScan laser flow cytometer (FACSCalibur, Becton-Dickinson, Franklin Lakes, NJ, USA). The data were analyzed using the software CELL Quest.

Apoptosis assay. Apoptosis was measured with caspase-3/7 assay (Promega, Madison, WI, USA) according to the manufacturer's protocol. Briefly, cells were seeded into a 96-well plate. After the treatment, 100 μ l of Apo-One Caspase-3/7 reagent was added to each well and was incubated at 37°C for 30 min. The fluorescence was measured at an excitation wavelength of 485 nm and an emission wavelength of 530 nm.

Enzyme-linked immunosorbent assay (ELISA). For the measurement of VEGF, 5x10⁵ U266 cells/well were seeded in 12-well plates and grown to 75-80% confluence, then cells were switched to fresh serum-free medium in the presence or absence of rosiglitazone and ATRA and incubated for another 12 h. Cell-free culture supernatants were harvested and assayed for secreted VEGF using commercially available ELISA kits (R&D Systems, Minneapolis, MN, USA).

Animal experiments. Male BALB/c-nu/nu mice (4-6 weeks old, Slac Laboratory Animal, Shanghai, China) were kept in the animal facilities at the Nanjing Medical University and maintained under specific pathogen-free conditions. All animal procedures were conducted according to the guidelines approved by the China Association of Laboratory Animal Care. Cultured HepG2 cells (5x10⁶) suspended in 0.2 ml PBS were injected into the right flank of mice. The mice were kept in a pathogen-free environment, 5-7 days later when the tumor volume reached 100 mm³, the mice were divided into four groups (control group and three-dose GYY4137 groups) in a manner to equalize the mean tumor among the four groups (n=7 each). GYY4137 at 50, 20 and 10 mg/kg dose suspended in 0.5% carboxymethyl cellulose (CMC) was given as gavage to mice daily for 4 weeks, and mice of control group were given 0.1 ml 0.5% CMC solution. The tumor size was measured in two orthogonal directions using calipers every three days, and the tumor volume (mm³) was estimated using the equation length x (width)² x 0.5. Four weeks later, the mice were sacrificed and the tumors were resected. Part of tumor tissues were homogenized and subjected to western blot assay. The primary antibodies were STAT3, p-STAT3 (Y705), p-STAT3 (S727), Bcl-2, Mcl-1, cyclin D1, survivin, HIF-1 α , VEGF (Cell Signaling Technology) and β -actin (Sigma).

Immunohistochemical (IHC) analysis. Immunohistology analysis was carried out using paraffin section. Paraffin section were incubated in a blocking solution (10% donkey serum + 5% non-fat dry milk + 4% BSA + 0.1% Triton X-100) for 10 min and then hydrated sections were incubated at 4°C overnight with anti-p-STAT3 (Y705) and p-STAT3 (S727) or anti-STAT3 antibody, respectively. After washing with PBS, the sections were incubated with diluted (1:200) biotinylated secondary antibody for 30 min. Subsequently, the slides were washed again in PBS and incubated for 30 min with the preformed avidin-horseradish peroxidase macromolecular complex. Development of peroxidase reaction was achieved by incubation in 0.01% 3,3-diaminobenzidine tetrahydrochloride.

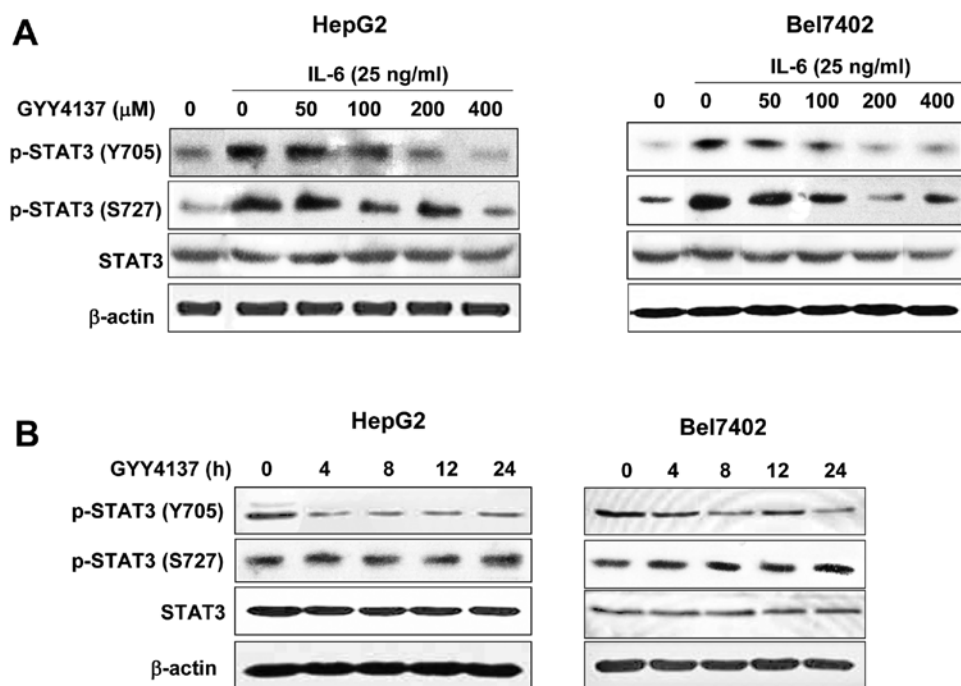


Figure 1. GYY4137 reduces the cell viability in human HCC cells by inhibiting IL-6/STAT3 signaling. (A) HCC cells were treated with the indicated concentrations of GYY4137 for 24 h and then induced by IL-6 for 15 min, after which whole-cell extracts were processed for western blot analysis using anti-p-STAT3 (Y705), anti-p-STAT3 (S727) and anti-STAT3 antibodies. (B) HCC cells were treated with the indicated concentrations of GYY4137 for 24 h and then induced by IL-6 for 15 min, after which whole-cell extracts were processed for western blot analysis using anti-p-STAT3 (Y705), anti-p-STAT3 (S727) and anti-STAT3 antibodies. β -actin served as a loading control.

ride (DAB) in PBS containing 0.01% hydrogen peroxide for approximately 5 min at room temperature. Sections were then washed thoroughly in tap water, counterstained in haematoxylin, dehydrated in absolute alcohol, cleared in xylene and mounted in synthetic resin for microscopic examination.

Statistical analysis. Statistical difference was analyzed by two-way Student's t-test. $P < 0.05$ was considered to indicate statistical significance. The values are expressed as the mean \pm SD. Three or more separates experiments were performed.

Results

GY4137 inhibits IL-6-induced STAT3 phosphorylation in HCC cells. To examine whether the antitumor activity of GYY4137 may be due to the inhibition of IL-6/STAT3 pathway, we evaluated the effects of GYY4137 on IL-6-induced STAT3 phosphorylation in human HCC cells. HepG2 and Bel7402 cell lines with higher IL-6 and phosphorylated STAT3 were treated with GYY4137 for 24 h. As shown in Fig. 1A, IL-6 significantly activated STAT3 phosphorylation at Y705 both in HepG2 and Bel7402 cells. GYY4137 inhibited the IL-6-induced p-STAT3 (Y705) in a dose-dependent manner, whereas it had no effect on p-STAT3 (S727) and total STAT3 (Fig. 1A). Furthermore, inhibition was evident as early as 4 h after treatment and lasted for 24 h (Fig. 1B) in HCC cell lines. These findings indicated that GYY4137 inhibited IL-6-induced STAT3 activation in human HCC cells.

GY4137 suppresses constitutive JAK2 activation and STAT3 downstream gene expression. JAK2 is considered as

one of the most common activators of STAT3. To explore the mechanism of the inhibitory effects on p-STAT3 (Y705), the levels of JAK2 phosphorylation were evaluated. P-JAK2 (Y1007/1008) was suppressed in HepG2 and Bel7402 cell lines with GYY4137 treatment, whereas basic JAK2 was not detectable (Fig. 2A). To further investigate whether GYY4137 would affect STAT3 downstream genes, we used western blot analysis to examine the expression of Bcl-2, Mcl-1, cyclin D1 and survivin. As shown in Fig. 2B, GYY4137 treatment downregulated the expression of these proteins both in HepG2 and Bel7402 cell lines.

GY4137 causes cell cycle arrest, suppresses cell viability and induces cell apoptosis. To examine the growth inhibitory effect of GYY4137, we first assessed cell cycle distribution by flow cytometric analysis. As shown in Fig. 3, GYY4137 increased the number of cells in the G0/G1 phase in HepG2 and Bel7402 cells. The results are consistent with the inhibitory effect of GYY4137 on cyclin D1 in these cells.

Since IL-6/STAT3 targets certain genes such as Bcl-2, Mcl-1 and survivin involved in anti-apoptosis, we next examined the effect of GYY4137 on apoptosis induction. As shown in Fig. 4A, GYY4137 promoted the cleavage of proapoptotic 116 kDa full-length PARP in an 89 kDa fragment, a process known to impair genomic integrity before apoptosis. We also observed that the levels of cleaved caspase-9 and caspase-3 were increased by treatment with GYY4137 in a dose-dependent manner (Fig. 4A). Flow cytometric data revealed that treatment with 200 and 400 μ M of GYY4137 increased the number of cells in the subG1 phase (13-20%), indicating that the HCC cells were undergoing apoptosis

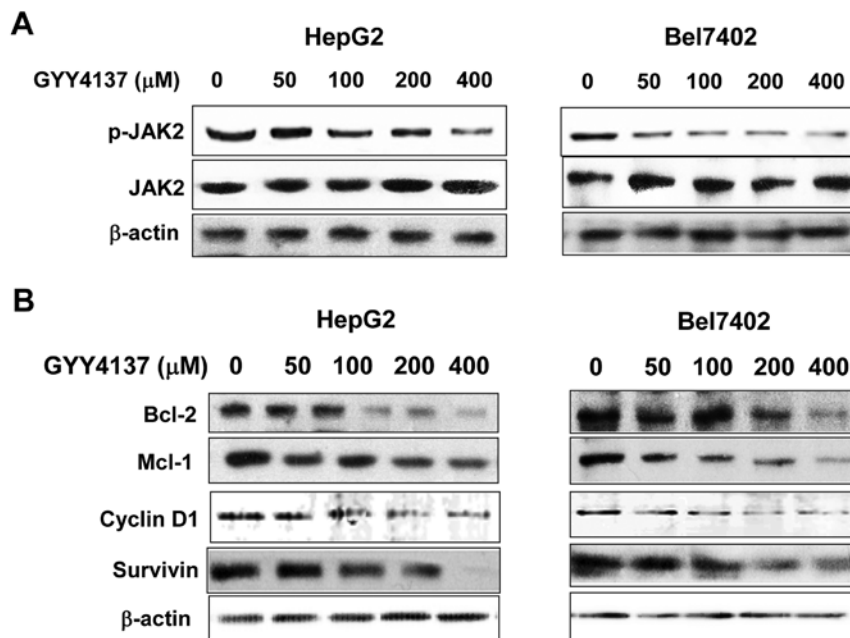


Figure 2. Effects of GYY4137 on constitutive JAK2 activation and STAT3 downstream gene expression. (A) HCC cells were treated with the indicated concentrations of GYY4137 for 24 h, after which whole-cell extracts were processed for western blot analysis using anti-p-JAK2 and anti-JAK2 antibodies. (B) HCC cells were treated with the indicated concentrations of GYY4137 for 24 h, after which whole-cell extracts were processed for western blot analysis using anti-Bcl-2, anti-Mcl-1, anti-cyclin D1 and anti-survivin antibodies. β -actin served as a loading control.

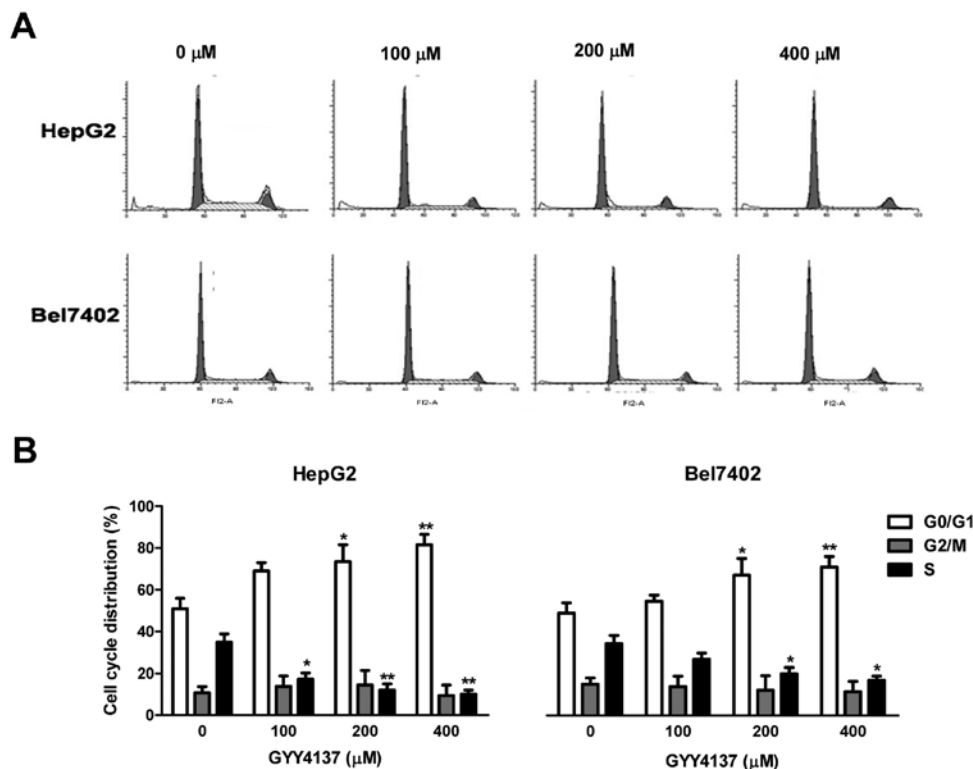


Figure 3. Effects of GYY4137 on cell cycle distribution in HepG2 and Bel7402 cells. (A) HepG2 and Bel7402 cells were treated with GYY4137 (50-400 μM) for 24 h, stained with PI and analyzed with a FACSCalibur flow cytometer. (B) Quantification of PI staining is presented as percentages corresponding to cell cycle distribution. Each value represents the mean \pm SD of triplicate wells. Statistical difference was analyzed by Student's t-test, * $P < 0.05$, ** $P < 0.01$ compared to control (0 μM of GYY4137).

(Fig. 4B). MTT assay showed that GYY4137 inhibited tumor cell viability time- and dose-dependently (Fig. 4C), while it

showed weak inhibition on normal hepatocellular LO2 cells only after 400 μM GYY4137 treatment for 72 h (data not

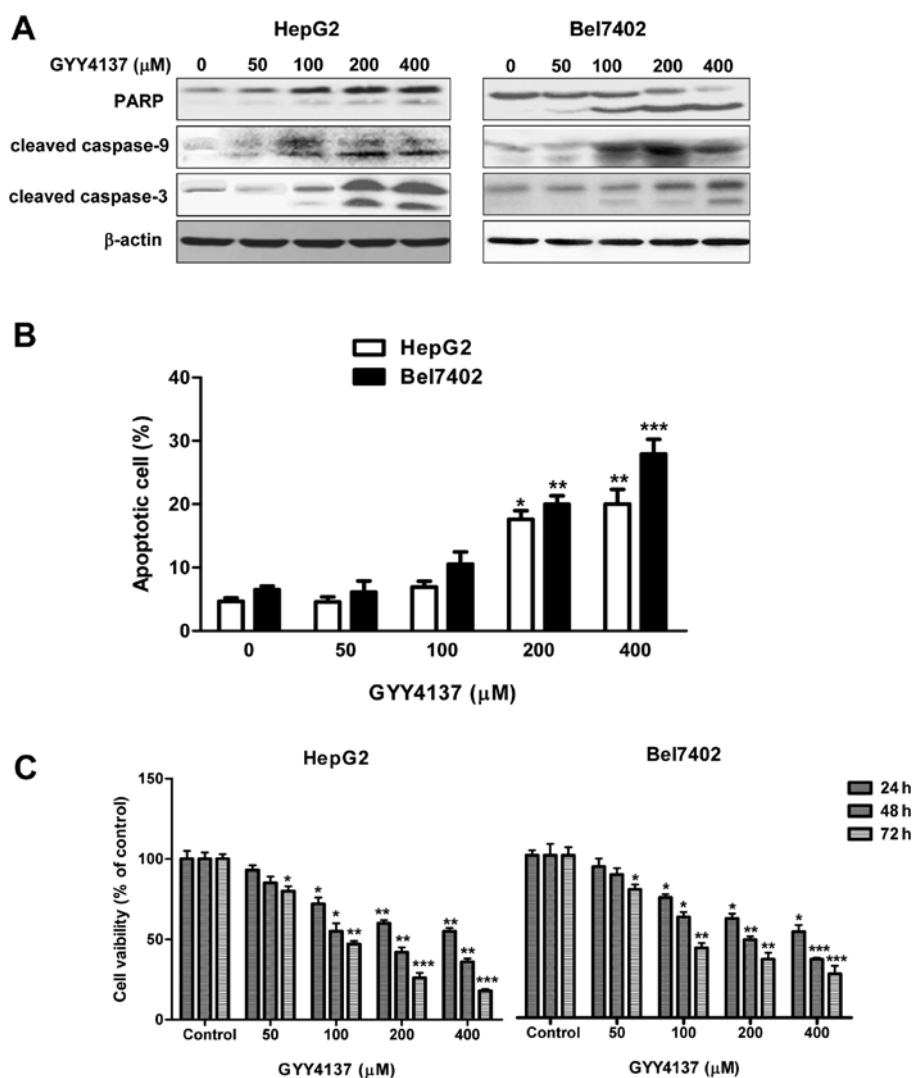


Figure 4. Effects of GYY4137 on apoptosis in HCC cells. (A) HepG2 and Bel-7402 cells were treated with indicated concentrations of GYY4137 for 24 h, after which whole-cell extracts were processed for western blot analysis using anti-cleaved-caspase 9, anti-cleaved-caspase 3 and anti-cleaved-PARP antibodies. β -actin served as a loading control. (B) HepG2 and Bel7402 were exposed to GYY4137 at the indicated concentration for 24 h, and the apoptotic assay was analyzed as sub-G1 percentage. Each value represents the mean \pm SD of triplicate wells. Statistical difference was analyzed by Student's t-test, * P <0.05, ** P <0.01 and *** P <0.001 compared to control (0 μ M of GYY4137). (C) HCC cells were treated with various concentrations of GYY4137 for 24, 48 and 72 h, and then subjected to MTT assay. Each value represents the mean \pm SEM of triplicate wells. Statistical difference was analyzed by Student's t-test, * P <0.05, ** P <0.01 and *** P <0.001 compared to control (0 μ M of GYY4137).

shown). These results showed that GYY4137 was able to induce apoptosis in HCC cells through regulating the caspase pathway.

GYY4137 inhibits expression of VEGF and HIF-1 α in HCC cells. A low oxygen level is a characteristic feature of solid tumors and a negative prognostic factor for cancer patient survival. The response of cancer cells to hypoxia not only drives neo-angiogenesis, but also enhances cancer cell survival and malignant phenotype development. Hypoxia is known to increase the expression of HIF-1 α , a major regulator of pro-angiogenic signaling. Since HIF-1 α is the major transcriptional modulator of angiogenic factors such as VEGF, we evaluated the effect of GYY4137 on hypoxia induced expression of HIF-1 α and VEGF in HCC cells. The cells were treated with various concentrations of GYY4137 under hypoxia mimicking condition induced by 100 μ M CoCl₂ for 6 h. As shown in Fig. 5A, GYY4137 suppressed the expression

of HIF-1 α , which was increased after exposure to hypoxia. To further confirm the effect of GYY4137 on hypoxia-induced VEGF, an immediate downstream target gene of HIF-1 α , VEGF protein level secreted to media was measured by ELISA in HepG2 cells. A notable increase of VEGF was observed under the hypoxic condition, whereas the treatment of GYY4137 suppressed VEGF production dose-dependently (Fig. 5B).

GYY4137 inhibits tumor growth in a subcutaneous HepG2 xenograft model. To determine the antitumor activity of GYY4137 *in vivo*, we evaluated its effect in a nude mouse xenograft model of HepG2 cells. GYY4137 was administered for 4 weeks. After 4 weeks, the mice were sacrificed and the tumor mass was dissected. The high dose of GYY4137 (50 mg/kg/d) inhibited tumor growth significantly (P <0.05) after administration for 13 days, and the low dose (10 mg/kg)

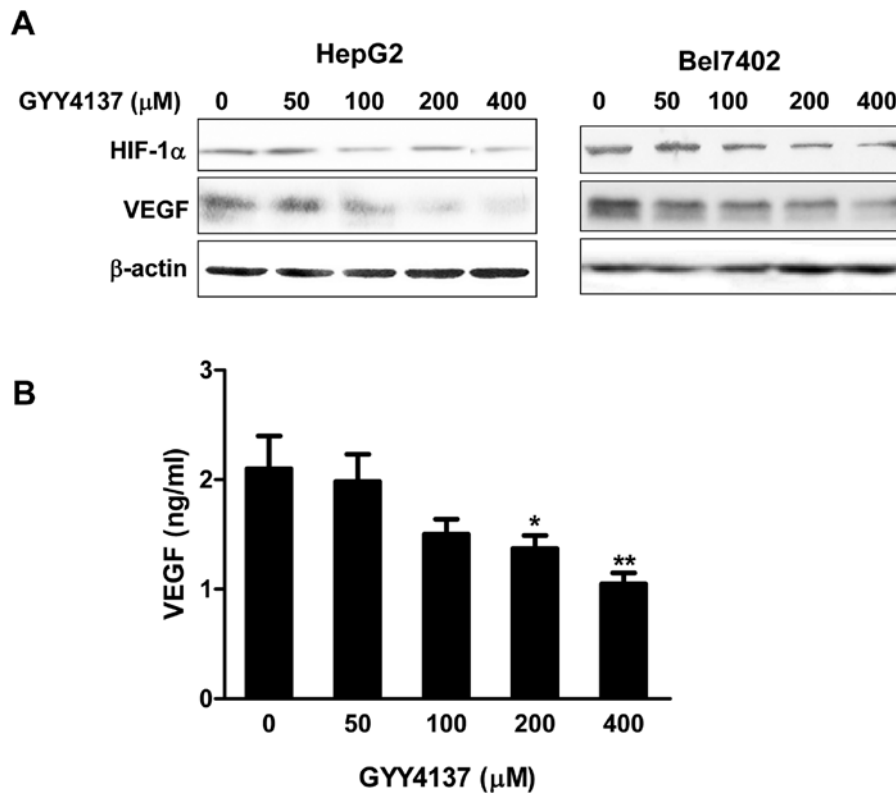


Figure 5. Effects of GYY4137 on VEGF and HIF-1 α expression in HCC cells. (A) HepG2 and Bel-7402 cells were treated with indicated concentrations of GYY4137 for 24 h under hypoxia mimicking condition induced by 100 μ M CoCl₂ for 6 h, after which whole-cell extracts were processed for western blot analysis using anti-VEGF and anti-HIF-1 α antibodies. β -actin served as a loading control. (B) Effect of GYY4137 on VEGF secretion in HepG2 cells. Cells were treated with the indicated concentrations of GYY4137 for 24 h, and supernatants were collected. The secreted level of VEGF was quantified by ELISA as described in Materials and methods. The bar graph represents the mean \pm SEM of six analyses. *P<0.05, **P<0.01 compared to the control.

of GYY4137 exhibited no significant inhibitory effect on tumor growth (Fig. 6A). Body weight of the mice was observed during administration of GYY4137. There was no significant weight loss in mice treated with GYY4137 of middle and high dose groups, while significant weight loss was detected in mice treated with GYY4137 of low dose or saline groups (Fig. 6B).

To confirm whether the inhibition of GYY4137 on xenograft tumor growth was mediated by blocking STAT3 signaling, we investigated the expression levels of p-STAT3 and STAT3 in xenograft tumor of mice treated with GYY4137 by IHC analysis. As shown in Fig. 7A and B, the level of p-STAT3 (Y705) was decreased in xenograft tumors of mice treated with GYY4137 compared with the model xenograft tumors, whereas the level of STAT3 had no significant change in the model group or the GYY4137 treated group. In concert with the decreased expression of p-STAT3, a clear downregulation in the target gene expression of STAT3, such as cyclin D1, Mcl-1, HIF-1 α and VEGF, were found in the xenograft tumor tissue of the GYY4137-treated mice, in a GYY4137 dose-dependent manner (Fig. 7C). Results *in vivo* further confirmed that the antitumor effect of GYY4137 was partly mediated by blocking the STAT3 signaling pathway.

Discussion

Clinical studies have indicated that constitutive STAT3 activation plays a critical role in tumor formation and devel-

opment in a variety of primary human cancers and cell lines, including HCC. Therefore, STAT3 signaling has emerged as an important therapeutic target for anticancer drug development (12,22). Aberrant activation of STAT3 may promote tumor cell proliferation through the upregulation of cyclin D1 and may suppress apoptosis through the upregulation of Bcl-2, Mcl-1 and survivin (10). Therefore, suppression of constitutively activated STAT3 not only induces apoptosis and radioresistance (23). The aim of this study was to investigate whether GYY4137 exerts its anticancer effect through inhibiting STAT3 signaling in HCC. We found that GYY4137 had anti-HCC effects and the underlying mechanism was associated with the inhibition of STAT3 signaling that led to the suppression of cancer cell proliferation by induction of cell cycle arrest, increased apoptosis and inhibition of angiogenesis *in vitro* and *in vivo*.

Phosphorylation of STAT3 at Y705 enables its dimerization, nuclear translocation, DNA binding and gene transcription (23), whereas phosphorylation of another conserved STAT3 residue, S727, enhances STAT3 transcriptional activity (24). Cooperation of tyrosine and serine phosphorylation is necessary for the full activation of STAT3 (25). Here, we showed that GYY4137 could inhibit IL-6-induced STAT3 activation in HCC cells by blocking JAK2 phosphorylation. STAT3 was constitutively phosphorylated at Y705 and S727 in HCC and GYY4137 inhibited phosphorylation of Y705 among HCC

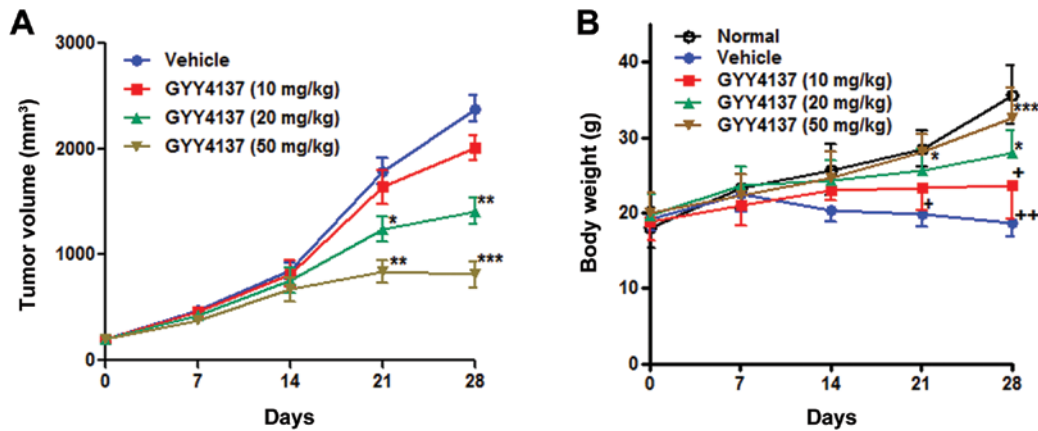


Figure 6. Effects of GYY4137 on tumor growth of nude mice bearing HepG2 xenograft tumors. (A) Tumor volume and (B) mouse body weight changes were determined every week during delivery period, statistical difference was analyzed by Student's t-test, the values are expressed as the mean volume of xenograft tumors \pm SEM. * $P < 0.05$, ** $P < 0.01$ and *** $P < 0.001$ compared to vehicle mice; * $P < 0.05$ and ** $P < 0.01$ compared to normal mice.

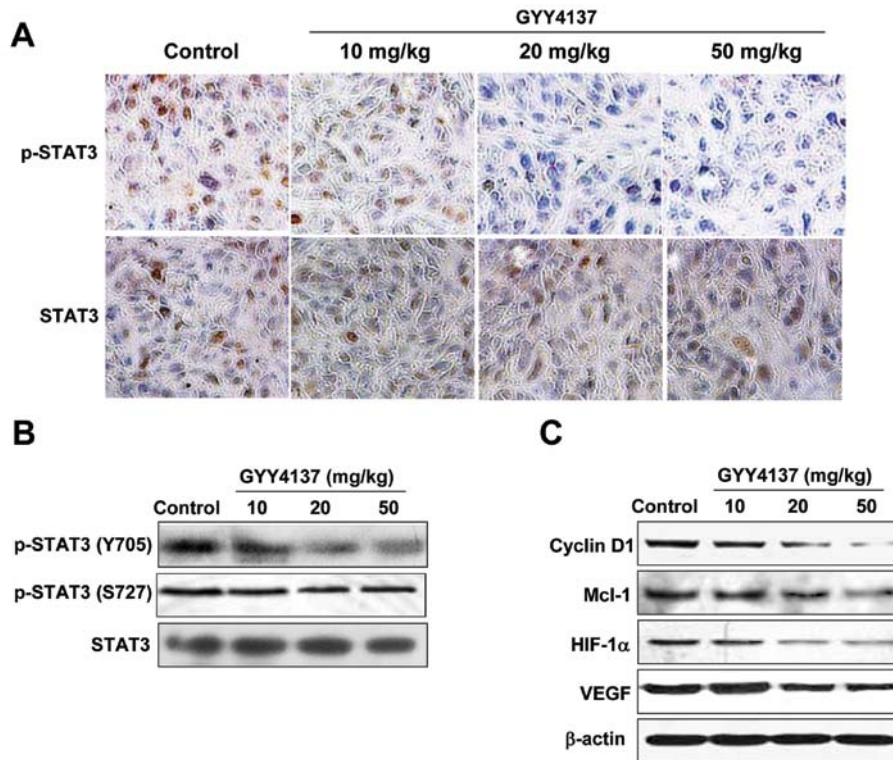


Figure 7. Effects of GYY4137 on STAT3 signaling in the xenografted HepG2 tumors of nude mice. (A) The xenografts in mice of model group and GYY4137 treatment groups were subjected to immunohistochemical analysis using p-STAT3 (Y705) or STAT3 antibodies. Positive cells are brown, negative cells are blue, magnification $\times 200$. (B) The xenograft tumor tissue in mice of model group and GYY4137 treatment groups were subjected to western blot analysis to determine the protein of anti-p-STAT3 (Y705) and anti-STAT3. (C) The xenografts in mice of the model group and GYY4137 treatment groups were subjected to western blot analysis to determine the protein of anti-cyclin D1, anti-Mcl-1, anti-HIF-1 α and anti-VEGF.

cells and HepG2 xenografts of nude mice that exhibited different molecular or genetic characteristics. The inhibition was evident as early as 4 h after treatment and lasted for 24 h, suggesting that the actions of GYY4137 are relatively rapid and prolonged. Moreover, we showed that GYY4137 downregulated STAT3 mediated downstream gene products involved in controlling cell cycle progression and programmed cell death (e.g., cyclin D1, Mcl-1, Bcl-2 and survivin) *in vitro* and *in vivo*.

Constitutively active STAT3 is associated with the induction of resistance to apoptosis possibly through the expression of Bcl-2 and cyclin D1 (26-28). Overexpression of Mcl-1 is found in a great percentage of HCC. Targeting Mcl-1 is a promising novel approach in HCC therapy (29). Therefore, downregulation of the expression of cyclin D1, Mcl-1, Bcl-2 and survivin was likely correlated with the ability of GYY4137 to facilitate apoptosis in HCC cells.

Apoptosis is a process of programmed cell death that serves as a major mechanism for the precise regulation of cell numbers and as a defense mechanism to remove unwanted cells (30). Mitochondria mediate apoptotic signaling via activation of the cell death initiator procaspase-9 (30,31). Activated caspase-9 in turn cleaves executioner caspase-3. The activated caspase-3 then cleaves PARP, a 116 kDa nuclear protein related to the process of programmed cell death (32). In addition, we observed that the antitumor activity of GYY4137 was also associated with the induction of apoptosis in HCC cells as indicated by *in vitro* evidence of increased cleaved caspase-9, caspase-3 and PARP cleavage. These results indicated that GYY4137 inhibited cell growth by regulating cell cycle progression and induced apoptosis in HCC cells.

VEGF and HIF-1 α are prominent transcriptional targets for STAT3 among the angiogenesis factors (10,33). HIF-1 α activation appears to be a very early event in carcinogenesis and this protein is expressed before histological evidence of angiogenesis or invasion (34,35). In regards to HCC, overexpression of HIF-1 α has been reported, which has been associated with a poor prognosis (36). Recently, both HIF-1 α and VEGF were identified to be involved in the malignant transformation of dysplastic liver nodules and additionally a hypoxia-independent overexpression of HIF-1 α has been shown to be involved in a model of mouse hepatocarcinogenesis (37). Suppression of HIF-1 α and STAT3 activity was demonstrated to inhibit the growth in HCC, ultimately leading to a reduction of tumor growth and vascularization *in vivo* (38). In the present study, we found that GYY4137 effectively inhibited VEGF and HIF-1 α expression in HCC cells and HepG2 xenografts of nude mice, which may be related with its inhibition of STAT3 activation. Therefore, downregulation of VEGF and HIF-1 α by GYY4137 may be of great significance in suppressing tumor cell invasion and metastasis.

In conclusion, GYY4137 blocks the STAT3 signaling pathway. The inhibition of STAT3 (Y705) phosphorylation triggered downregulation of gene products related to cell survival, cell cycle progression, thus in turn triggered cell apoptosis and cell cycle arrest. Importantly, GYY4137 exhibited antitumor effect in the HepG2 xenograft nude mouse model. These results suggested that GYY4137 is a potential candidate for treatment of HCC.

Acknowledgements

This study was supported by a grant from the Priority Academic Program of Jiangsu Higher Education Institutions (JX10231801).

References

- Bruix J, Sherman M; Practice Guidelines Committee, American Association for the Study of Liver Diseases: Management of hepatocellular carcinoma. *Hepatology* 42: 1208-1236, 2005.
- Villanueva A, Newell P, Chiang DY, Friedman SL and Llovet JM: Genomics and signaling pathways in hepatocellular carcinoma. *Semin Liver Dis* 27: 55-76, 2007.
- Llovet JM and Bruix J: Novel advancements in the management of hepatocellular carcinoma in 2008. *J Hepatol* 48 (Suppl 1): S20-S37, 2008.
- Niu G, Wright KL, Huang M, *et al*: Constitutive Stat3 activity up-regulates VEGF expression and tumor angiogenesis. *Oncogene* 21: 2000-2008, 2002.
- Real PJ, Sierra A, De Juan A, Segovia JC, Lopez-Vega JM and Fernandez-Luna JL: Resistance to chemotherapy via Stat3-dependent overexpression of Bcl-2 in metastatic breast cancer cells. *Oncogene* 21: 7611-7618, 2002.
- Wang T, Niu G, Kortylewski M, *et al*: Regulation of the innate and adaptive immune responses by Stat-3 signaling in tumor cells. *Nat Med* 10: 48-54, 2004.
- Schindler C, Levy DE and Decker T: JAK-STAT signaling: from interferons to cytokines. *J Biol Chem* 282: 20059-20063, 2007.
- Alvarez JV, Febbo PG, Ramaswamy S, Loda M, Richardson A and Frank DA: Identification of a genetic signature of activated signal transducer and activator of transcription 3 in human tumors. *Cancer Res* 65: 5054-5062, 2005.
- Bollrath J, Phesse TJ, von Burstin VA, *et al*: gp130-mediated Stat3 activation in enterocytes regulates cell survival and cell-cycle progression during colitis-associated tumorigenesis. *Cancer Cell* 15: 91-102, 2009.
- Garcia R, Bowman TL, Niu G, *et al*: Constitutive activation of Stat3 by the Src and JAK tyrosine kinases participates in growth regulation of human breast carcinoma cells. *Oncogene* 20: 2499-2513, 2001.
- Liu Y, Liu A, Li H, Li C and Lin J: Celecoxib inhibits interleukin-6/interleukin-6 receptor-induced JAK2/STAT3 phosphorylation in human hepatocellular carcinoma cells. *Cancer Prev Res (Phila)* 4: 1296-1305, 2011.
- Yang J, Cai X, Lu W, *et al*: Evodiamine inhibits STAT3 signaling by inducing phosphatase shatterproof 1 in hepatocellular carcinoma cells. *Cancer Lett* 328: 243-251, 2013.
- Gu FM, Li QL, Gao Q, *et al*: Sorafenib inhibits growth and metastasis of hepatocellular carcinoma by blocking STAT3. *World J Gastroenterol* 17: 3922-3932, 2011.
- Rajendran P, Ong TH, Chen L, *et al*: Suppression of signal transducer and activator of transcription 3 activation by butein inhibits growth of human hepatocellular carcinoma *in vivo*. *Clin Cancer Res* 17: 1425-1439, 2011.
- Calvisi DF, Ladu S, Gorden A, *et al*: Ubiquitous activation of Ras and Jak/Stat pathways in human HCC. *Gastroenterology* 130: 1117-1128, 2006.
- Hu LF, Wong PT, Moore PK and Bian JS: Hydrogen sulfide attenuates lipopolysaccharide-induced inflammation by inhibition of p38 mitogen-activated protein kinase in microglia. *J Neurochem* 100: 1121-1128, 2007.
- Rose P, Moore PK, Ming SH, Nam OC, Armstrong JS and Whiteman M: Hydrogen sulfide protects colon cancer cells from chemopreventative agent beta-phenylethyl isothiocyanate induced apoptosis. *World J Gastroenterol* 11: 3990-3997, 2005.
- Lee ZW, Zhou J, Chen CS, *et al*: The slow-releasing hydrogen sulfide donor, GYY4137, exhibits novel anti-cancer effects *in vitro* and *in vivo*. *PLoS One* 6: e21077, 2011.
- Li L, Fox B, Keeble J, *et al*: The complex effects of the slow-releasing hydrogen sulfide donor GYY4137 in a model of acute joint inflammation and in human cartilage cells. *J Cell Mol Med* 17: 365-376, 2013.
- Takada Y, Ichikawa H, Badmaev V and Aggarwal BB: Acetyl-11-keto-beta-boswellic acid potentiates apoptosis, inhibits invasion, and abolishes osteoclastogenesis by suppressing NF-kappa B and NF-kappa B-regulated gene expression. *J Immunol* 176: 3127-3140, 2006.
- Isomoto H, Mott JL, Kobayashi S, *et al*: Sustained IL-6/STAT3 signaling in cholangiocarcinoma cells due to SOCS-3 epigenetic silencing. *Gastroenterology* 132: 384-396, 2007.
- Won C, Lee CS, Lee JK, *et al*: CADPE suppresses cyclin D1 expression in hepatocellular carcinoma by blocking IL-6-induced STAT3 activation. *Anticancer Res* 30: 481-488, 2010.
- Aggarwal BB, Kunnumakkara AB, Harikumar KB, *et al*: Signal transducer and activator of transcription-3, inflammation, and cancer: how intimate is the relationship? *Ann NY Acad Sci* 1171: 59-76, 2009.
- Lufe C, Koh TH, Uchida T and Cao X: Pin1 is required for the Ser727 phosphorylation-dependent Stat3 activity. *Oncogene* 26: 7656-7664, 2007.
- Aziz MH, Manoharan HT, Church DR, *et al*: Protein kinase Cepsilon interacts with signal transducers and activators of transcription 3 (Stat3), phosphorylates Stat3Ser727, and regulates its constitutive activation in prostate cancer. *Cancer Res* 67: 8828-8838, 2007.
- Selvendiran K, Kuppusamy ML, Ahmed S, *et al*: Oxygenation inhibits ovarian tumor growth by downregulating STAT3 and cyclin-D1 expressions. *Cancer Biol Ther* 10: 386-390, 2010.

27. Ai T, Wang Z, Zhang M, *et al*: Expression and prognostic relevance of STAT3 and cyclin D1 in non-small cell lung cancer. *Int J Biol Markers* 27: e132-e138, 2012.
28. Zhang K, Pang B, Xin T, *et al*: Increased signal transducer and activator of transcription 3 (STAT3) and decreased cyclin D1 in recurrent astrocytic tumours compared with paired primary astrocytic tumours. *J Int Med Res* 39: 2103-2109, 2011.
29. Sieghart W, Losert D, Strommer S, *et al*: Mcl-1 overexpression in hepatocellular carcinoma: a potential target for antisense therapy. *J Hepatol* 44: 151-157, 2006.
30. Bossy-Wetzel E and Green DR: Apoptosis: checkpoint at the mitochondrial frontier. *Mutat Res* 434: 243-251, 1999.
31. Estaquier J, Vallette F, Vayssiere JL and Mignotte B: The mitochondrial pathways of apoptosis. *Adv Exp Med Biol* 942: 157-183, 2012.
32. Wurstle ML, Laussmann MA and Rehm M: The central role of initiator caspase-9 in apoptosis signal transduction and the regulation of its activation and activity on the apoptosome. *Exp Cell Res* 318: 1213-1220, 2012.
33. Wei D, Le X, Zheng L, *et al*: Stat3 activation regulates the expression of vascular endothelial growth factor and human pancreatic cancer angiogenesis and metastasis. *Oncogene* 22: 319-329, 2003.
34. Zhu H, Feng Y, Zhang J, *et al*: Inhibition of hypoxia inducible factor 1alpha expression suppresses the progression of esophageal squamous cell carcinoma. *Cancer Biol Ther* 11: 981-987, 2011.
35. Matsuyama T, Nakanishi K, Hayashi T, *et al*: Expression of hypoxia-inducible factor-1alpha in esophageal squamous cell carcinoma. *Cancer Sci* 96: 176-182, 2005.
36. Yasuda S, Arai S, Mori A, *et al*: Hexokinase II and VEGF expression in liver tumors: correlation with hypoxia-inducible factor 1 alpha and its significance. *J Hepatol* 40: 117-123, 2004.
37. Tanaka H, Yamamoto M, Hashimoto N, *et al*: Hypoxia-independent overexpression of hypoxia-inducible factor 1alpha as an early change in mouse hepatocarcinogenesis. *Cancer Res* 66: 11263-11270, 2006.
38. Moser C, Lang SA, Mori A, *et al*: ENMD-1198, a novel tubulin-binding agent reduces HIF-1alpha and STAT3 activity in human hepatocellular carcinoma (HCC) cells, and inhibits growth and vascularization in vivo. *BMC Cancer* 8: 206, 2008.